

STUDY OF AERODYNAMIC CHARACTERISTICS OF AN AIRCRAFT DURING APPROACH TO LANDING IN A DISTURBED ATMOSPHERE

Victor V. Vyshinsky¹, Doan Cong Chinh^{2,*}

¹Central Aerohydrodynamic Institute (TsAGI), Zhukovskiy, Russia

²Moscow Institute of Physics and Technology (State University), Dolgoprudny, Russia

*E-mail: doancongchinh@phystech.edu

Received: 26 November 2021 / Published online: 22 April 2022

Abstract. An approximate method is proposed for determining the aerodynamic effect of coherent vortex structures (CVS) of atmospheric turbulence on an aircraft. As a source of the CVS the vortex wind wakes arising when the atmospheric wind flows around the mountain massif of the Son Tra peninsula, located near the Da Nang airport, and the vortex wake behind the Su-27 type aircraft in the landing configuration are considered. Modeling the formation of a vortex structure is carried out by the grid method within the framework of the boundary value problem for the Reynolds-averaged Navier–Stokes equations. The evolution and stochastics of the far wake are modeled in a two-dimensional approximation by discrete Rankine vortices. The assessment of the increment of forces and moments from the effect of the vortex system on the aircraft was carried out within the framework of the panel method. The situation is considered when a light transport aircraft gets into a vortex wake behind an aircraft with a swept wing and a passenger aircraft of the MS-21 type, approaching for landing at the CVS from a mountainous terrain.

Keywords: coherent vortex structures in the atmosphere, flight safety, Reynolds-averaged Navier–Stokes equations, computational fluid dynamics, boundary element method.

1. INTRODUCTION

When flowing around a mountain landscape and large structures with a wind boundary layer, coherent vortex structures (CVS) arise, which can cross the glide path and the airspace area near the airport. The source of the CVS is also an aircraft. He caught in a vortex structure undergoes significant changes in aerodynamic forces and moments, which is especially dangerous near the ground. Getting into the CVS can lead to engine stalling, asymmetric stall on the wing and entry into a spin [1]. Ignorance of the state

and behavior of the atmosphere over mountainous terrain and the unavailability of pilots to fly in conditions of orographic turbulence (ORT) can lead to flight accidents and disasters.

For a seaside airport, coastal winds play a significant role, the behavior of which is complicated by the presence of mountainous terrain [2,3]. The model of the atmospheric boundary layer over a complex surface in the presence of breeze circulation is considered in [4]. The location of the mountain airfield near the sea is complicated by high air humidity. The flow around a mountain ridge, accompanied by a rapid change in pressure and temperature, leads to condensation of steam [5] and an increase in atmospheric turbulence due to the release of energy.

For strict problem statement, the flow parameters at the boundary of the computational domain are determined within the framework of the mesoscale atmospheric model (COSMO-RU07 [6]), in which, at the first step, an area with a characteristic size of about ten thousand km is calculated on a grid with a cell of 20 km. In this case, the boundary conditions are selected using the global quasi-static atmosphere model GME of the German Meteorological Service or the global IFS model of the European Center of Medium-Range Forecasts [7]. At the next step, a subdomain with a characteristic size of about a thousand km is calculated on a grid with a cell of 7 km, then on an even finer grid with a cell of 1 km in an area of about a hundred km.

In this paper, two cases are considered: 1) hit of the light transport aircraft in the vortex wake of the Su-27 aircraft [8] in the landing configuration; 2) hit of a passenger aircraft in the CVS, which arose during the wind flow around a mountainous terrain, during the landing approach. In order to verify the calculation method used to simulate the formation of the CVS, a model problem of the flow around a building in the form of a parallelepiped is considered.

The circle of distributions in the study of the CVS can be divided into three zones. 1) The region of the CVS generator: analytical approaches are impossible in this region, numerical methods are used within the framework of boundary value problems (BVP). At the same time, it should be remembered that due to the lack of sufficiently reliable near-wall models of turbulence and unsolved, in general, the problem of flow separation, all these methods are not rigorous. 2) The problem of the dynamics of the CVS. The most powerful research tool developed here is the analytical one. However, models operating with vortex filaments are non-physical [9,10] - the internal structure of the core is needed. They do not take into account the influence of the atmosphere, in particular, its turbulence, stratification, and wind. Mathematical simulation taking into account viscosity rests on the absence of models of free turbulence. 3) The problem of diffraction of

a vortex on an obstacle (hit of an aircraft in CVS). Here, both analytical approaches are possible (the mathematical model can be reduced to a trivial one, retaining the physics of the phenomenon), and modeling methods within the framework of BVP and engineering techniques. This raises the question of the correctness of the approaches used within the studied zones.

2. APPROXIMATE SOLUTION METHOD

Due to the complexity of the problem being solved, a simplified zonal method is proposed. The problem is solved in the approximation of an incompressible gas, flow scales are chosen at which one can neglect the non-inertiality of the coordinate system and use Boussines isotropic turbulence models.

The components of the method are: a) modeling of the formation of the CVS, for which the BVP is solved for the Reynolds-averaged Navier–Stokes equations (RANS); b) formation of the initial two-dimensional vortex structure; c) simulation of the evolution and stochastics of the CVS, taking into account the decrease in circulation; d) calculation of the increment of forces and moments arising on the aircraft from the impact of the CVS using a computer code created on the basis of the boundary element method.

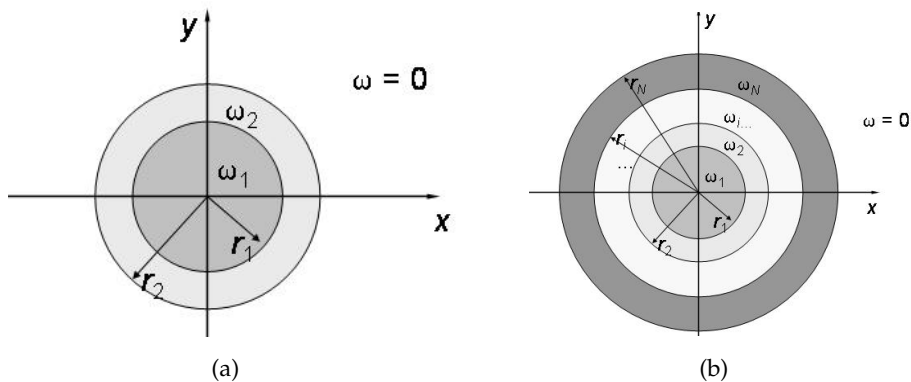


Fig. 1. Vorticity distributions in the cores of two-layer (a) and n -layer (b) potential vortices

The following algorithm for approximating the initial field in the cores of discrete Rankine vortices is proposed and implemented. Fig. 1 shows the vorticity distributions in two-layer and n -layer potential vortices. A certain number of maxima ω_{\max} and minima ω_{\min} are specified. In the vicinity of the extrema in the iterative procedure $R_v^{n+1} = R_v^n + h$, where h is the local step of the computational grid, R_v is the radius of the circle centered at the extremum, at each step the vorticity flow inside the circle with the radius R_v^n is

summed, and by Stokes' theorem

$$\Gamma = 2\pi R_v V_\tau = \int \int_{C_v} \omega_z dx dy,$$

the value of the velocity V_τ of the tangent to the contour of the boundary C_v of the region of integration (circle of radius R_v^n) is determined. Reaching the maximum V_τ (Fig. 2) allows one to determine the radius of the core R_v . In the case of a single-layer vortex $R_v^n = a$, circulation $\Gamma = 2\pi a V_\tau$, vorticity in the core $\omega = \Gamma / (\pi a^2)$. In the case of a two-layer potential vortex $R_v^n = r_2$, $R_v^{n-1} = r_1$, $V_\tau^n = V_2$, $V_\tau^{n-1} = V_1$ and by formulas (1) $\omega_1 = 2V_1/r_1$, $\omega_2 = (2V_2r_2 - 2V_1r_1)/(r_2^2 - r_1^2)$.

$$V(r) = \begin{cases} [\omega_1/2] \cdot r, & 0 \leq r \leq r_1 \\ [(\omega_1 - \omega_2) \cdot r_1^2/2] \cdot \frac{1}{r} + [\omega_2/2] \cdot r, & r_1 < r \leq r_2 \\ [\omega_1 \cdot r_1^2/2 + \omega_2/2 \cdot (r_2^2 - r_1^2)] \cdot \frac{1}{r}, & r > r_2 \end{cases} \quad (1)$$

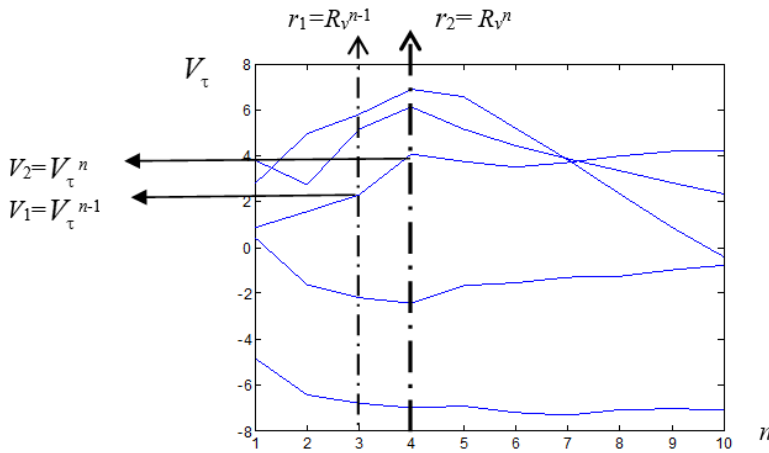


Fig. 2. The character of convergence V_τ in the iterative procedure $R_v^{n+1} = R_v^n + h = (n + 1)h$

3. SIMULATION OF THE FORMATION OF THE CVS

To simulate the CVS behind the aircraft, a BVP is solved for RANS with a two-parameter $k-\omega$ SST closure model. An airplane Su-27 is considered in the landing configuration (with flaperon and leading edge deflection angles of 18° and 30° , respectively), flying without sideslip $\beta = 0$ at a speed of 70 m/s at an angle of attack $\alpha = 11^\circ$. The calculation is performed for half of the space with a longitudinal vertical plane of symmetry. Atmosphere parameters: air temperature 295.5 K, pressure 95600 Pa, density 1.127 kg/m³. The calculation is carried out at an average level of turbulence, 8000 iterations

were performed with a time step: $dt = 0.0005$ s, the results are given at the time $t = 4$ s. The boundaries of the computational domain along the X axes: $-100 \div 730$ m, Y: $-100 \div 100$ m and Z: $0 \div 100$ m.

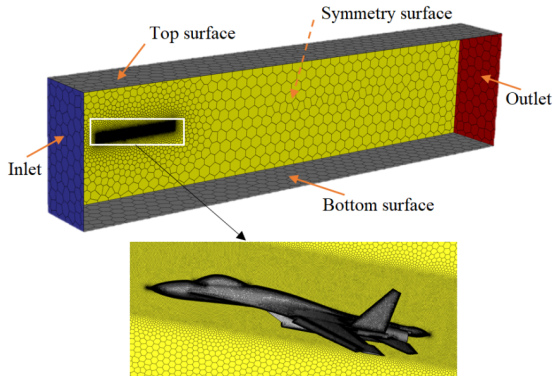


Fig. 3. Fragments of the computational grids

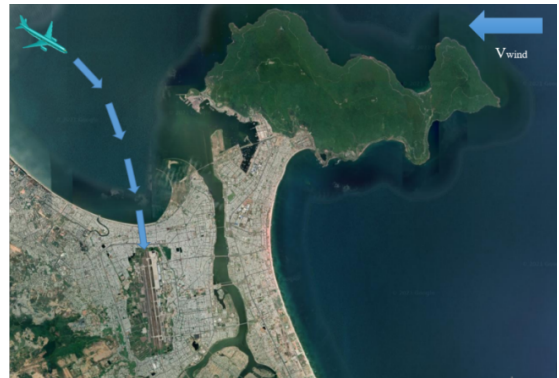


Fig. 4. The airport scheme

The calculation was performed on a mesh with 15,603,231 nodes, generated using the ANSYS FLUENT software package (MIPT license No. 1079611). Fig. 3 shows the fragments of the computational grids. Fig. 4 shows a scheme of the airport in Da Nang city (Vietnam). The airport has two parallel runways 35R–17L and 35L–17R, oriented at angles of 350° and 170° , respectively.

The view of the computational domain and the surface of the peninsula is shown in Fig. 5. Boundaries of the modelling area along the X axes: $-8000 \div 20,000$ m, Y: $-8800 \div 17,600$ m and Z: $0 \div 2000$ m (the upper surface of the computational domain is hidden).

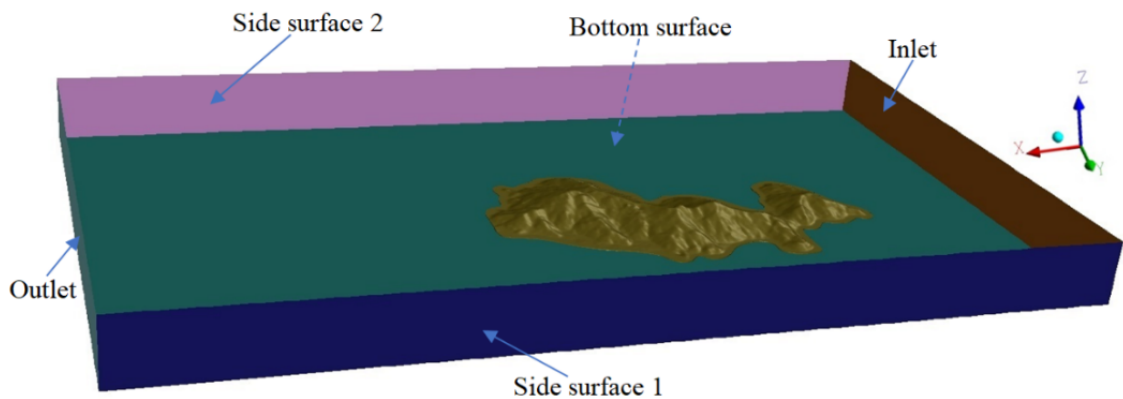


Fig. 5. View of the computational area and the surface of the peninsula

The number of grid nodes: 18,195,550. The z -axis is directed upwards, the x -axis is in the direction of the wind, and the y -axis is orthogonal to the other two axes and forms a right-hand triplet. Fig. 6 shows fragments of the computational grids.

At the output of the computational domain, the average static pressure is set equal to atmospheric; on the underlying surface - no-slip conditions; at the upper and lateral boundaries - no-penetration conditions. At the input boundary, velocity and temperature profiles along the height are set (Fig. 7).

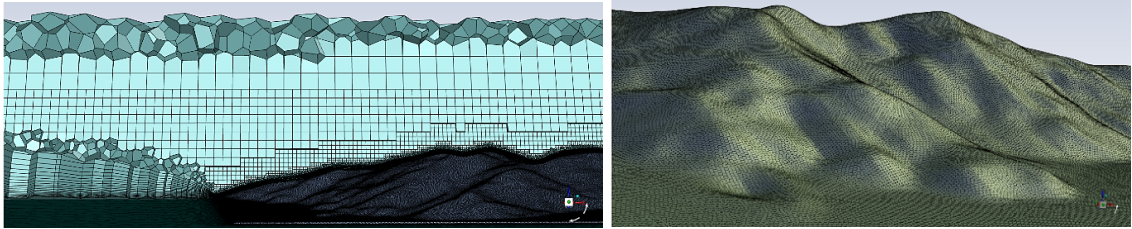


Fig. 6. Fragments of computational grids

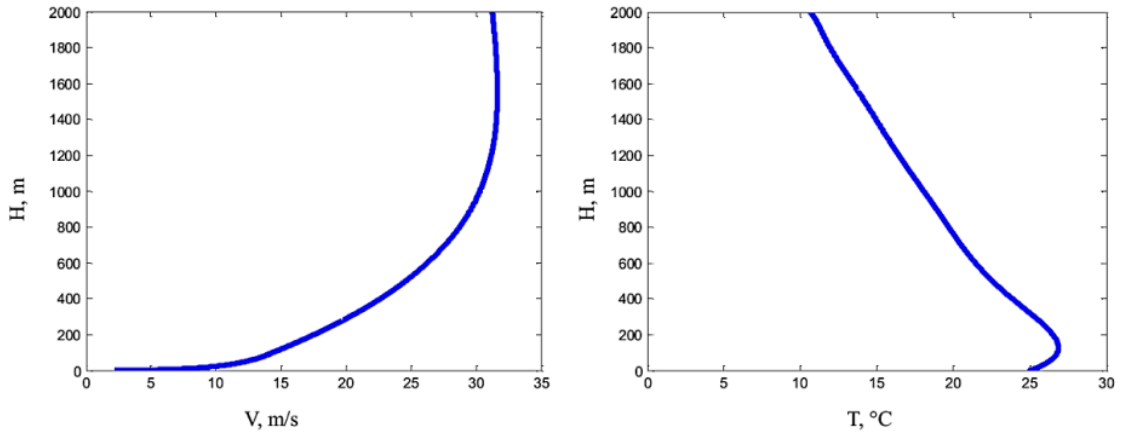


Fig. 7. Wind speed and temperature profile with altitude

4. MODELING OF FORMATION OF CVS AND VERIFICATION OF SOLUTIONS

In order to verify the method for solving BVP for RANS equations with a two-parameter SST closure model, a building in the form of a parallelepiped located near the runway (RW) was considered in [11]. The wind flow perpendicular to the runway has a linear velocity profile

$$u(y) = \begin{cases} U_{\infty} \times y/300, & y \leq 300 \\ U_{\infty}, & y \geq 300 \end{cases}$$

In numerical simulation, it should be kept in mind that the correctness of the solved BVPs is not proven. The problem set can be solved under different boundary conditions [12]. In order to choose the correct boundary conditions, the following model problems in the approximation of an inviscid incompressible gas were considered: the generalized Dirichlet BVP for the Poisson equation $\Delta\Psi = \omega$ with respect to the stream function Ψ :

$$u = \frac{\partial\Psi}{\partial y}, \quad v = -\frac{\partial\Psi}{\partial x}, \quad \Psi_b = \Psi_a + \int_a^b -v \cdot dx + u \cdot dy,$$

along with the vorticity transfer equation

$$\omega = \frac{\partial v}{\partial x} - \frac{\partial u}{\partial y}, \quad \frac{\partial\omega}{\partial t} + u \frac{\partial\omega}{\partial x} + v \frac{\partial\omega}{\partial y} = 0,$$

and the generalized Neumann problem for the Laplace equation with respect to the potential $\Delta\varphi = 0$ in the three-dimensional (3D) case.

In the first case, the alternative statements are the mixed BVP (which is also correct) and in the second case, the problem involves soft boundary conditions (SBCs) at the outflow boundary. It should be noted that both problems show a loss of mass at the outflow boundary.

The statement of the generalized Dirichlet problem is shown in (2)

$$\begin{aligned} \psi_{x=0}(y) = \psi_{x=15}(y) &= U_\infty \begin{cases} y^2/6, & y \leq 3 \\ (y-3/2), & y \geq 3 \end{cases} \\ \omega_{x=0} = \omega_{x=15} &= -\frac{\partial u}{\partial y} = \begin{cases} -U_\infty/3, & y \leq 3 \\ 0, & y > 3 \end{cases} \end{aligned} \quad (2)$$

The flows at the inflow and outflow boundaries are the same. To solve it, a Cartesian orthogonal mesh was used with square cells $h_x = h_y = 0.05$ (where the number of nodes was 301×121). The Gauss–Seidel relaxation algorithm with the relaxation parameter 0.8 was used to solve the Poisson equation, and the Lax scheme was used to solve the vorticity transport equation. Then, 50,000 iterations were carried out at time step $\Delta t = 0.0001$, and 10 relaxations were performed at each iteration. The total mass flux $J = \int_0^6 u(y) dy$ was equal to $J_{in} = 90.495$ and $J_{out} = 90.493$ at the inflow and outflow boundaries, respectively, and the deficit was equal to $\Delta J = -0.0018$. The calculation on a coarse mesh (where $h_x = h_y = 0.1$, and the number of nodes was 151×61) gave $J_{in} = 90.978$, $J_{out} = 90.974$ and $\Delta J = -0.0045$.

A mixed BVP was considered as the second case for these equations, where the soft conditions were set at the outflow boundary

$$\left. \frac{\partial \Psi}{\partial x} \right|_{x=15} = 0, \quad \left. \frac{\partial \omega}{\partial x} \right|_{x=15} = 0.$$

In this case, the equations degenerate at the outflow boundary

$$\frac{\partial^2 \Psi}{\partial y^2} = \omega, \quad \frac{\partial \omega}{\partial t} + v \frac{\partial \omega}{\partial y} = 0.$$

In order to solve it, the same numerical scheme (mesh, algorithms, and number of iterations) was used. The total mass flux at the inflow boundary was the same. At the outflow boundary $J_{out} = 90.4126$; the deficit was 50 times higher, which amounted to $\Delta J = -0.0824$.

To solve the generalized Neumann BVP and the mixed problem for the Laplace equation in the 3D case, a single $15 \times 6 \times 10$ computational domain and a $151 \times 61 \times 101$ mesh were taken. 10^6 iterations of the relaxation process were carried out with a relaxation parameter of 0.8. In contrary to the two-dimensional problem, in this case, the flow is potential, and the velocity profile at the inflow and outflow boundaries is written as $u_{x=0}(y) = u_{x=15}(y) = U_\infty$ (the Neumann problem).

If the Neumann conditions are replaced by a soft condition at the outflow boundary $\frac{\partial \varphi}{\partial x} \rightarrow \text{const}$, $\Rightarrow \frac{\partial^2 \varphi}{\partial x^2} = 0$ then the law of conservation of mass is violated. This is due to the parabolization of the Laplace equation. The total mass flux at the inflow boundary was $J_{in} = 2997$, at the outflow boundary $J_{out} = 2877$ (deficit $\Delta J = 120$) for the case of the Neumann problem and $J_{out} = 147$ (deficit $\Delta J = 2853$) for the case of the mixed BVP. The results obtained show that the BVPs with SBCs, which lead to the degeneration of the continuity equation $\text{div} \vec{V} = 0$, the loss of mass at the outflow boundary, and the parabolization of convective terms in the momentum equation at the boundary with soft conditions

$$\frac{\partial \vec{V}}{\partial t} + \nabla \vec{V} \vec{V} = -\frac{1}{\rho} \nabla p + \frac{\mu}{\rho} \Delta \vec{V}.$$

Considering the obtained result, the BVP was solved for the RANS equations using the following boundary conditions: soft conditions were set on the upper boundary; symmetry conditions were set on the lateral surfaces; no-slip conditions were set on the underlying surface, including the landscape and architectural objects; and hard boundary conditions (HBCs) were set at the outflow boundary. The computational meshes in the section $z = \text{const}$, obtained by successive doubling, had 30,000, 120,000, and 480,000 nodes.

In order to validate the method, a series of calculations was carried out for a building that has the shape of a non-circular cylinder (Fig. 8). The oncoming flow has a surface wind profile. To carry out the calculations, a block structured grid was built with a prismatic sublayer on the earth’s surface, consisting of 20 cells, having a height of the first cell of 0.01 m and a cell growth rate of 1.2. The total volume of the grid is 5 million cells, and about half of them are in the prismatic sublayer. When solving the problem, all variables are reduced to a dimensionless form. The calculation was carried out until the values of the integral averaged loads reached the stationary values. $D = 27$ m, $V_\infty = 20$ m/s are taken as the characteristic linear size and speed, so that the number $Re = 2.7 \times 10^7$. For such values, the flow is self-similar in terms of Reynolds numbers. The calculation was carried out for five wind directions.



Fig. 8. Full-scale building and model in scale 1 : 130 in the Wind tunnel

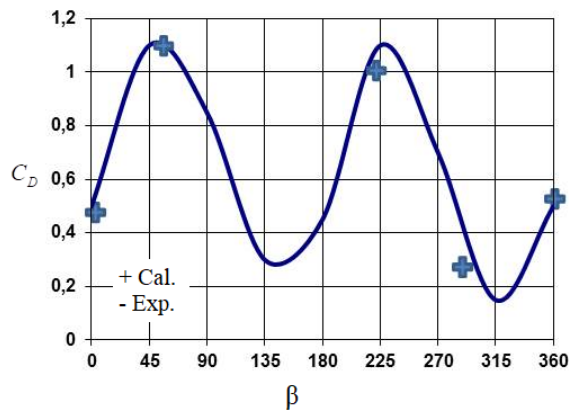


Fig. 9. Dependence $C_D(\beta)$

The results of the calculation and experiment are shown in Fig. 9, C_D - drag coefficient of the building and β - wind direction. Satisfactory agreement is observed.

4.1. CVS modelling results for the aircraft Su-27

Figs. 10–11 show the results of the calculation in the section $x = \text{const}$ at a distance of half the wingspan from the aircraft.

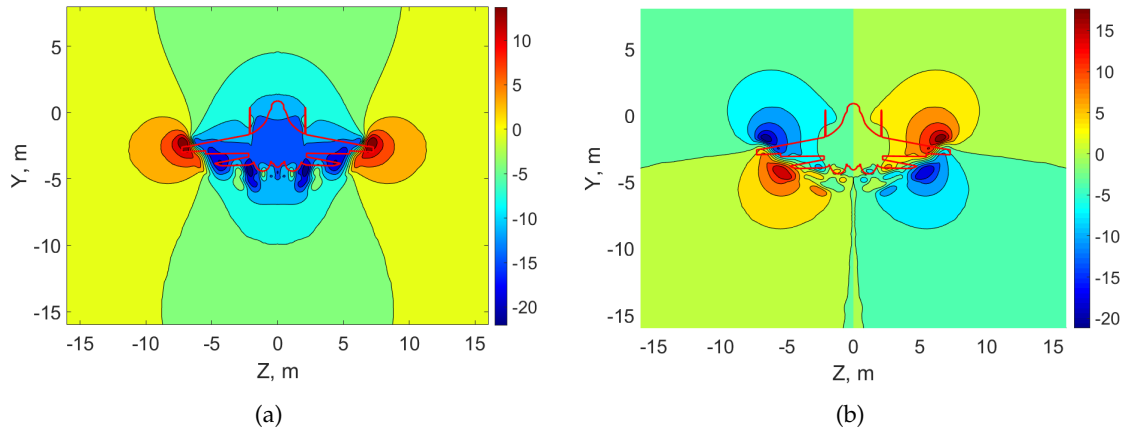


Fig. 10. Fields of the vertical (a) and horizontal (b) components of the velocity in the section $x = 7.5$ m

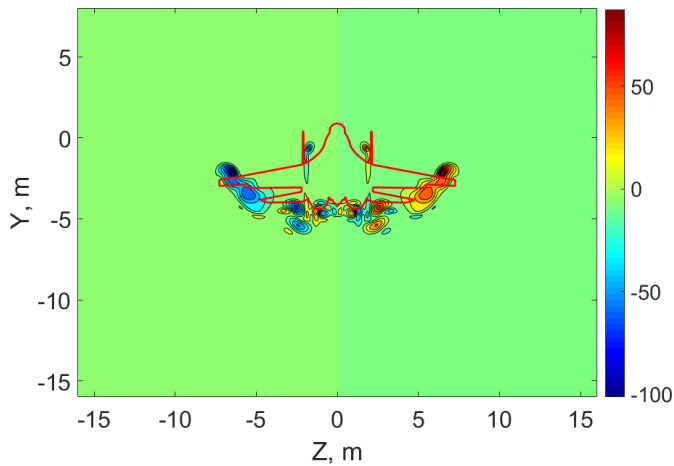
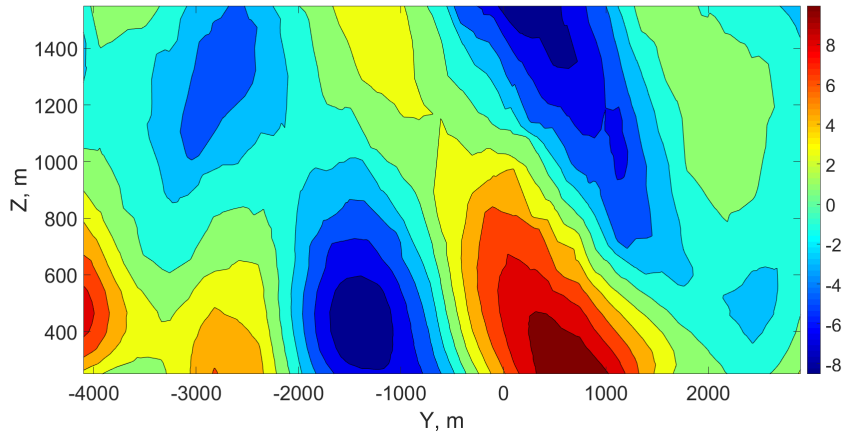


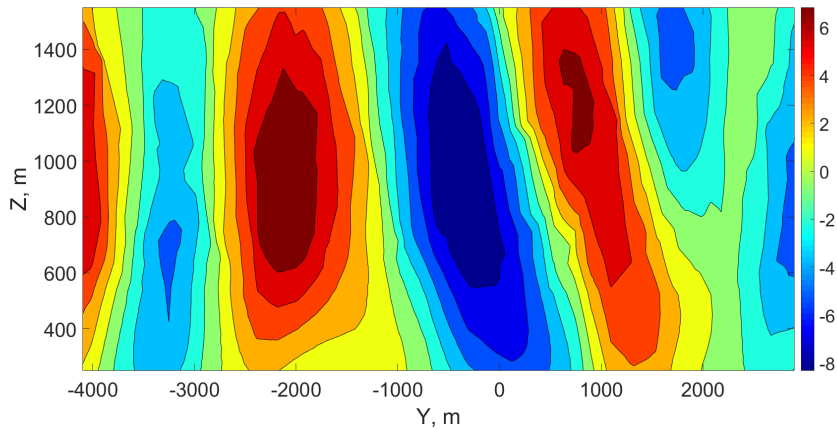
Fig. 11. The field of the longitudinal vorticity component in the section $x = 7.5$ m

4.2. The results of modelling the formation of the CVS for the mountain range

Fig. 12 shows the fields of the transverse velocity components in control section, at distances of 6500 m from the peninsula. These results were used to model the evolution of CVS, described in Paragraph 6.



(a) Horizontal component of the velocity



(b) Vertical component of the velocity

Fig. 12. The fields of the transverse velocity components in the section $x = 6500$ m from the peninsula

5. CRITERIA FOR INDEPENDENT VERIFICATION OF SOLUTIONS

The methods of computational fluid dynamics implement the solution of initial-boundary value problems for nonlinear equations in partial derivatives, the correctness

of which has not been proven [12] on computers, as a rule, of insufficient power for their full verification. To verify the methods for calculating stationary flows in [13], criteria were proposed based on the principle of maximum pressure [14], according to which the surfaces

$$Q = 0.5 \left(\overline{\overline{\Omega}}_{ij} \overline{\overline{\Omega}}_{ij} - \overline{\overline{S}}_{ij} \overline{\overline{S}}_{ij} \right) = 0,$$

divide the flow region into subregions, where $Q > 0$, in which there can be no local pressure maximum, and $Q < 0$, where there can be no local minimum. Here

$$\overline{\overline{\Omega}}_{ij} = 0.5 \left(\partial u_i / \partial x_j - \partial u_j / \partial x_i \right) - \text{vorticity tensor},$$

$$\overline{\overline{S}}_{ij} = 0.5 \left(\partial u_i / \partial x_j + \partial u_j / \partial x_i \right) - \text{symmetric tensor of strain rates}.$$

Since there is a rarefaction in the core of the vortex, otherwise the vortex would not exist, and the separation region is characterized by a reduced pressure, then $Q < 0$ testifies a violation of the principle of maximum pressure. On this basis, Criteria 1 and 2 were proposed in [13], requiring the positivity of Q in vortex cores and flow separation regions. The presence of regions containing many fragments $Q < 0$ in the formation zone of vortex structures testifies a violation of the local isotropy of the flow and, as a consequence, the incorrectness of linear models of gradient diffusion, which reduces the accuracy of the closure models. Based on this, Criterion 3 was proposed, which requires the absence of sharp oscillations of Q in the flow region. Criterion 4 requires that the flow field does not have closed surfaces $Q = 0$, enclosing the streamlined body or its fragments (ring structures), since they necessarily intersect the wake behind the body, containing the regions of minimum pressure of separation zones and vortex structures.

6. MODELING OF EVOLUTION AND STOCHASTICS OF CVS

Fig. 13(a) shows the initial two-dimensional coherent structure of a wake of 3 + 3 vortices behind an aircraft of the Su 27 type at a distance of half the wingspan. The positions, radii and circulation of vortices are equal, respectively, $Y_{vort} = -2.15, -4.3, -3.45$, $Z_{vort} = 6.5, 2.55, 5.5$; $R_{vort} = 0.55, 0.45, 0.8$; $G_{vort} = 46.0, 24.12, 73.02$. Fig. 13(b) shows the initial two-dimensional coherent structure of the wake of 2 vortices in the section $x = 100$ m behind the aircraft. The structure of the wake in the Rankine vortex approximation has the following form: vortex radii $R_{vort} = 2.37; 2.37$, their circulation $G_{vort} = -123.13; 123.13$, their position in the section $x = 100$ m horizontally $Z_{vort} = -4.57; 4.57$ and vertical $Y_{vort} = -8.0; -8.0$.

When modeling the evolution of the formed CVS, a decrease in circulation of the circulation is taken into account. For $q = 1$ m/s the following formula was proposed

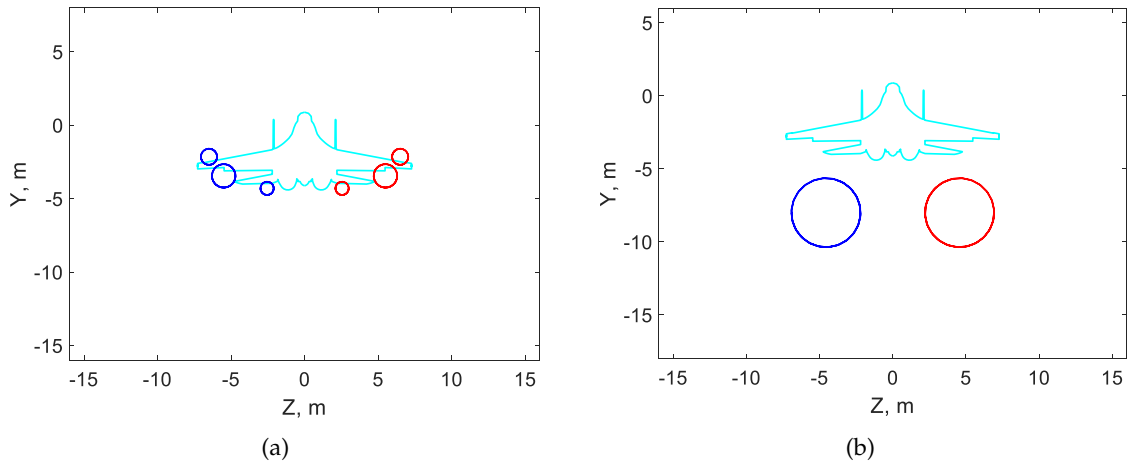


Fig. 13. Initial two-dimensional vortex structure

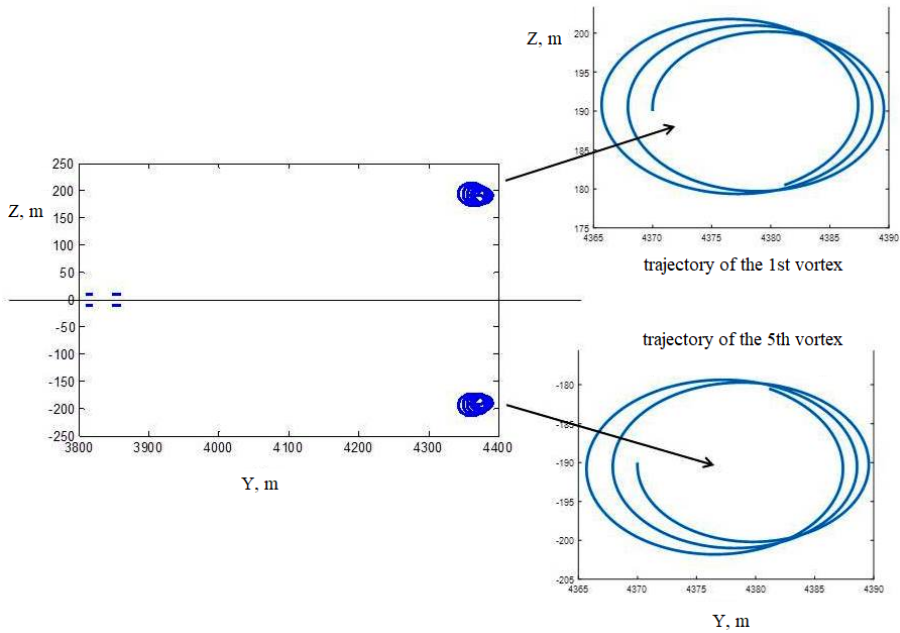


Fig. 14. Evolution of coherent vortex structures from 4 + 4 vortices during 20 s in the section $x = \text{const}$

in [15]

$$\Gamma(t) = \Gamma_0 K(t), \quad K(t) = A + B/t^m,$$

where the constants $A = 200, B = 1400, m = 0.9$.

The evolution of the CVS is modeled in the form of a two-dimensional vortex structure in the potential approximation by discrete vortices with a core of a two-layer Rankine vortex.

The evolution of the vortex system arising from the wind flow around the Son Tra peninsula is simulated for 100 s (1000 steps with a time step $dt = 0.1$ s). Fig. 14 shows a fragment of the evolution of the CVS, consisting of 4 pairs of vortices on the section $x = \text{const}$ for 20 s. The trajectories of the first and antisymmetric fifth vortices are given separately. Evolving, the system of vortices is transported by the wind.

The evolution of a CVS consisting of 4 pairs of vortices is shown in Fig. 15. Evolving, it is transported by the wind towards the runway.

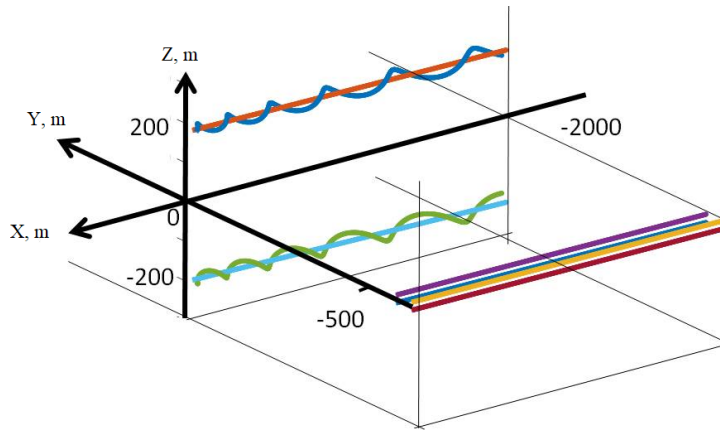


Fig. 15. CVS evolution from 4 + 4 vortices within 20 s

7. CALCULATION OF THE INCREMENT OF FORCES AND MOMENTS ARISING ON THE PLANE FROM THE IMPACT OF THE CVS

The assessment of the impact of the CVS on the aircraft hitting it is carried out using a computer code created on the basis of the boundary element method [16].

The surface of the body is divided into panels (Fig. 16), within which the intensity of the double layer is constant. The disturbed velocity field is modelled by a finite sum of Rankine vortices. The velocity induced by these vortices in the center of each panel is sought, and, based on the no-penetration condition, the vortex circulation along the perimeter of the panel is found, which is equivalent to a double layer of sources on the panel.

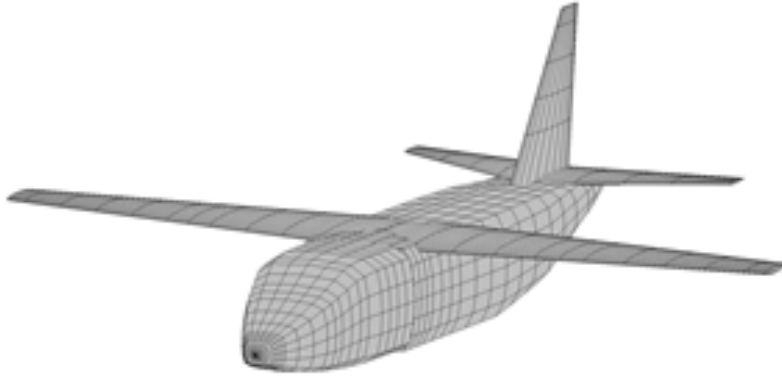


Fig. 16. Airplane “Bityug” (partitioning scheme on the panel)

A twin-engine light transport aircraft “Bityug” with an increased level of wing bearing properties is considered as a flying aircraft under conditions of rotary turbulence. The aerodynamic layout (Fig. 16) is made according to the “high-wing” scheme with a “deck” arrangement of the tail unit [17].

To validate computer code, in [15] the calculation results were compared with the experimental data obtained in the wind tunnel T-103 at TsAGI. The model is made on the scale of 1 : 6.5 in relation to the full-scale aircraft. The tests were carried out at a flow velocity $V = 50$ m/s ($M \approx 0.15$), corresponding to the number $Re \approx 1 \times 10^6$, along the average aerodynamic chord of the wing. When calculating the coefficients of aerodynamic (drag C_D , lift C_L , cross C_C) forces and (rolling C_l , yawing C_n , pitching C_m) moments, the area, the average aerodynamic chord and the wingspan of the model were taken as characteristic dimensions.

To make the flow structure in the wind tunnel test section similar to that in the vortex structure two-section tapered wing capable of differentially deflecting the half-wings installed at the wing-tunnel nozzle exit [18]. The model in a vortex flow experiences significant changes in the values and behavior of the rolling moments and yawing moments, as well as the lift force. The presented experimental results agree satisfactorily with the calculation results.

The situation is considered when the “Bityug” aircraft gets into the centers of the vortices generated by the Su-27 aircraft.

Table 1 shows the results of calculating the increments of forces and moments acting on the aircraft in sections $x = 7.5$ m and $x = 100$ m. Table 1 shows that there is an area in which the induced yawing moment exceeds the available $\Delta C_{n.av} = 0.045$. It can also be seen that the found maximum induced yawing moment in the second case (the initial

Table 1. Increments of the aerodynamics forces and moments coefficients

Relative position of aircraft, m	ΔC_D	ΔC_L	ΔC_C	ΔC_l	ΔC_n	ΔC_m
$x = 7.5$ m						
$\Delta y = -2.15, \Delta z = 6.5$	-0.006	0.6452	0.1255	-0.00041	0.0271	-0.1997
$\Delta y = -4.3, \Delta z = 2.55$	0.000051	-0.1041	0.3430	0.0271	0.0672	-0.0488
$\Delta y = -3.45, \Delta z = 5.5$	0.00076	0.189	0.2036	0.0013	0.0469	-0.1711
$x = 100$ m						
$\Delta y = -8, \Delta z = 4.57$	0.0039	0.1141	0.1671	-0.0169	0.0338	-0.0366
$\Delta y = -8, \Delta z = 0$	0.0011	0.0019	0.3253	-0.0327	0.0605	-0.0053

cross-section of the formation of a two-dimensional CVS $x = 100$ m) $\Delta C_n = 0.605$ is close to the value of 0.672 obtained in the first case (the initial cross-section of the formation of a two-dimensional CVS $x = 7.5$ m).

As a second example, the approach to the landing of the MS-21 type aircraft [19] on the runway of the Da Nang International Airport (Vietnam) from the sea is considered. Near the airport is the peninsula Son Tra - the source of the CVS. It is assumed that the wind has the same course angle. In this case, the surface of the aircraft is divided into 876 panels (Fig. 17).

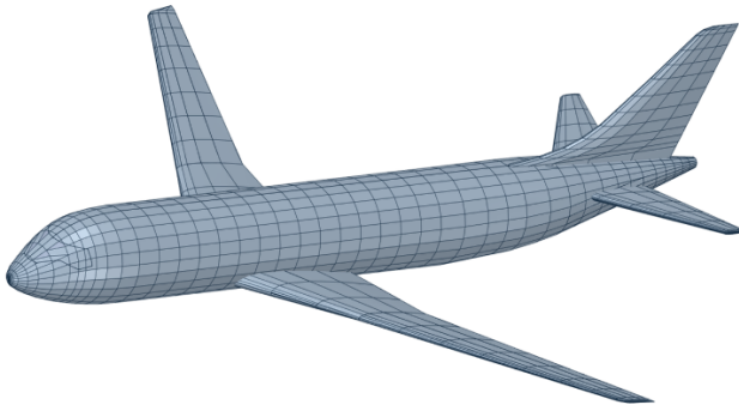


Fig. 17. Aircraft MS-21 type (partitioning scheme on the panels)

On Fig. 18, the results of calculating the increment of aerodynamic forces and moments for different altitudes (from 100 to 500 m) of the aircraft's entry into the CVS are given. On the abscissa axis, a lateral deviation along the y -axis is laid in the range from -500 to 1500 m. The fan of curves corresponds to different altitudes of the aircraft.

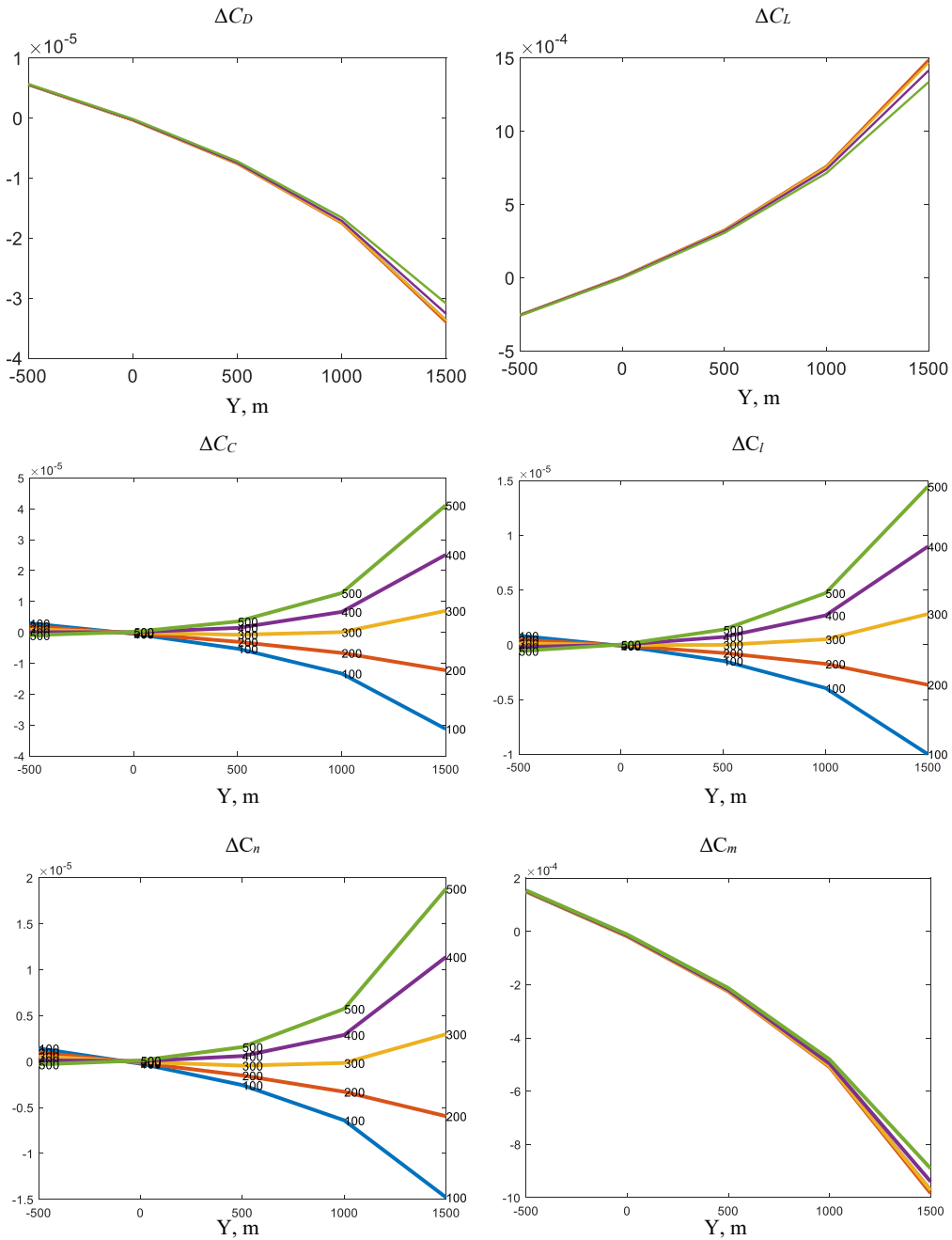


Fig. 18. Increments of coefficients of aerodynamic forces and moments depending on the flight altitude and lateral deviation of the aircraft

The maximum available rolling moment of the MS-21 type aircraft with a full deflection of the ailerons is $|\Delta C_{l_{av}}| = 0.05$, and the available value of the yawing moment when

the rudder is deflected by an angle of 25° $|\Delta C_{n_{av}}| = 0.04$. As can be seen, the induced rolling and yawing moments do not exceed the available control moments.

8. DISCUSSION OF THE OBTAINED RESULTS AND CONCLUSIONS

In a strict statement, the solution to this problem consists in modeling the state of the atmosphere along the flight path of the aircraft with the subsequent calculation of its flow around the non-potential flow of the disturbed atmosphere and, using the found pressure distribution on the surface, to determine the increment of forces and moments. At the same time, one cannot neglect the reverse influence of the aircraft on the CVS. The solution of the problem in this statement requires not only colossal computer resources, but also a huge array of boundary data, which is difficult, and sometimes impossible to obtain.

The created approximate method can be used to simulate dangerous situations associated with an aircraft hitting coherent vortex structures of a disturbed atmosphere, as well as to search for means of increasing flight safety when organizing traffic in the airport area, in particular, in take-off and landing modes under conditions of orographic turbulence. The method will be useful when looking for measures to expand the capabilities of aviation when flying in mountainous terrain, as well as when simulating complex situations in the operation of ship-based aircraft and unmanned aircraft.

A preliminary analysis of hazardous situations associated with hitting the CVS from engineering structures would be useful in making decisions about their construction.

Implementation of the created model on flight simulators will help prepare pilots for hazardous situations when flying in airspace over a mountainous landscape. The created model can be used to assess the impact of ORT on combat effectiveness; development of recommendations for updating the flight manual; taking into account the influence of ORT on the carrying capacity of a mountain airfield; determining the effect of ORT on pilot fatigue.

REFERENCES

- [1] A. V. Bobylev, V. V. Vyshinsky, G. G. Soudakov, and V. A. Yaroshevsky. Aircraft vortex wake and flight safety problems. *Journal of Aircraft*, **47**, (2010), pp. 663–674. <https://doi.org/10.2514/1.46432>.
- [2] G. R. Barri. *Weather and climate in the mountains*. L.: Gidrometeoizdat, 311 p., (1984). (in Russian).
- [3] S. S. Zilitinkevich. *The dynamics of the atmospheric boundary layer*. L.: Hydrometeorological Publishing, 292 p., (1970). (in Russian).

- [4] L. P. Bykov. The application of the atmosphere boundary layer model above the complex surface to the study of breeze circulation. In *Proceedings of the Main Geophysical Observatory*, Vol. 454, (1981), pp. 97–108. (in Russian).
- [5] D. L. Laikhtman. *The physics of the atmospheric boundary layer*. L.: Gidrometeoizdat, 341 p., (1970). (in Russian).
- [6] G. S. Rivin, I. A. Rozinkina, A. N. Bagrov, and D. V. Blinov. The mesoscale model COSMO-RU 07 and the results of its operational tests. In *Information Collection*, Vol. 39, (2012), pp. 15–48.
- [7] D. Majewski, D. Liermann, P. Prohl, B. Ritter, M. Buchhold, T. Hanisch, G. Paul, W. Wergen, and J. Baumgardner. The operational global icosahedral–hexagonal gridpoint model GME: Description and high-resolution tests. *Monthly Weather Review*, **130**, (2002), pp. 319–338. [https://doi.org/10.1175/1520-0493\(2002\)130<0319:togihg>2.0.co;2](https://doi.org/10.1175/1520-0493(2002)130<0319:togihg>2.0.co;2).
- [8] <https://grabcad.com/library/su-27-2017-model-edf-70mm-1>.
- [9] T. O. Aubakirov, A. I. Zhelannikov, P. E. Ivanov, and M. I. Nisht. *Tracks and their impact on aircraft*. Modeling on the computer, Almaty, 280 p., (1999). (in Russian).
- [10] A. S. Ginevsky and A. I. Zhelannikov. *Vortex wakes of aircraft*. In Moscow: FIZMATLIT, 172 p., (2008). (in Russian).
- [11] V. V. Vyshinsky and K. T. Zoan. Numerical simulation of the flow around landscape fragments and solution verification. *TsAGI Science Journal*, **51**, (6), (2020), pp. 641–650. <https://doi.org/10.1615/tsagiscij.2021037822>.
- [12] P. Roach. *Computational fluid dynamics*. M.: Mir, 616 p., (1980).
- [13] V. Anikin, V. Vyshinsky, O. Pashkov, and E. Streltsov. Using the maximum pressure principle for verification of calculation of stationary subsonic flow. *Herald of the Bauman Moscow State Technical University. Series Mechanical Engineering*, (2019), pp. 4–16. <https://doi.org/10.18698/0236-3941-2019-6-4-16>.
- [14] V. V. Vyshinsky and G. B. Sizykh. The verification of the calculation of stationary subsonic flows and the presentation of results. *Mathematical Models and Computer Simulations*, **11**, (2019), pp. 97–106. <https://doi.org/10.1134/s2070048219010162>.
- [15] V. V. Vyshinsky and K. T. Zoan. Aircraft aerodynamics in a disturbed atmosphere. *Proceedings of Moscow Institute of Physics and Technology*, **13**, (2), (2021), pp. 40–48. https://doi.org/10.53815/20726759_2021_13_2_40.
- [16] Y. N. Sviridenko and Y. L. Ineshin. Application of the panel method with symmetrization of features to the calculation of the flow around an aircraft, taking into account the influence of engine jets. In *Proceedings of TsAGI*, number 2622, (1996), pp. 41–53. (in Russian).
- [17] Y. S. Mikhailov. Modeling the impact of a vortex wake on an aircraft model in a wind tunnel. *Scientific Bulletin of MSTU GA*, (175), (2012), pp. 62–69. (in Russian).

- [18] Y. S. Mikhailov. Vortex wake simulation in a wind tunnel. In *Proceedings of TsAGI*, number 2641, (1999), pp. 197–203.
- [19] <https://3dwarehouse.sketchup.com/model/2d7562f5bf2c7f2da1d85548168d6015/template-irkut-ms-21-original-by-saelin-wip-2mb>.